Biochemical and crystallographic study of Hyd-2 type [NiFe]-hydrogenase from *Citrobacter* sp. S-77.

「酸素安定性[NiFe]ヒドロゲナーゼの構造化学」

2016

NOOR DINA MUHD NOOR

Leading Program in Doctoral Education

Graduate School of Life Science

University of Hyogo

兵庫県立大学大学院生命理学研究科

博士課程教育リーディング大学院

論文内容の要旨

論 文 題 目　　Biochemical and crystallographic study of Hyd-2 type [NiFe]-hydrogenase from *Citrobacter* sp. S-77.
「酸素安定性[NiFe]ヒドロゲナーゼの構造化学」

論文提出者　Noor Dina Muhd Noor

Hydrogenase catalyze the reversible conversion of molecular hydrogen to proton and electrons. These enzymes are potentially relevant to biotechnological applications because when H_2 is used as a fuel in combination with O_2, only water is produced, and it does not cause any ambient pollution. The most abundant hydrogenases contain a [NiFe] active site; these proteins are generally biased towards hydrogen oxidation activity and are reversibly inhibited by oxygen. Membrane bound type [NiFe]-hydrogenase from *Citrobacter* sp. S-77 (CS-77) possesses a strong hydrogen oxidation activity. It was also observed to have high oxygen- and thermo-stability which leads a potential ability for application to an efficient catalyst in H_2-based biotechnology. The purification procedure of Hyd-2 type [NiFe]-hydrogenase from CS-77 was improved by applying a treatment of trypsin before chromatography. Both the purified protein samples with and without trypsin treatment were successfully crystallized by using the sitting drop vapor diffusion method and polyethylene glycol as a precipitant. Both crystals belonged to the space group P21, with unit cell parameters of $a = 63.90$, $b = 118.89$, $c = 96.70$ Å, $\beta = 100.61$ ° for the protein subjected to trypsin treatment, and $a = 65.38$, $b = 121.45$, $c = 98.63$ Å, $\beta = 102.29$ ° for the sample not treated with trypsin. The crystal obtained from the trypsin-treated protein diffracted to 1.60 Å, which is considerably better than the 2.00 Å resolution obtained without trypsin treatment. The [NiFe]-hydrogenase from *Citrobacter* sp. S-77 retained catalytic activity with some amount of O_2, indicating that it has clear O_2 tolerance.

Contents

1.0 Introduction

1.1 Hydrogenases

Hydrogenases catalyze the reversible oxidation of molecular hydrogen to protons and electrons according to the reaction: $H_2 \longleftrightarrow 2H^+ + 2e^-$. This reaction plays a vital role in anaerobic metabolisms of a wide variety of microorganisms. Most of these enzymes are found in Archea and Bacteria, and a few in Eucarya (Vignais *et al.*, 2001). Three phylogenetically distinct classes of hydrogenases have been characterized. They can be distinguished by their metal content in the active site: nickel-iron ([NiFe]-), di-iron ([FeFe]-) and mono-iron ([Fe]-) hydrogenases. Among them, [NiFe]-hydrogenases represent the largest class.

1.2 [NiFe]-hydrogenase

[NiFe]-hydrogenases can be classified based on molecular phylogeny that divides them into four groups; Group 1 contains "standard" periplasmic hydrogenases and membrane-bound (MBH) H_2 uptake hydrogenases; Group 2 contains uptake hydrogenase and sensory hydrogenases; Group 3 contains F_{420}-reducing, $NAD(P)^+$-reducing, methylviologen-reducing, and bidirectional $NAD(P)^+$-reducing hydrogenases; and Group 4 contains energy-converting hydrogenases (Figure 1). Periplasmically oriented H_2-uptake [NiFe]-hydrogenases which belong to Group 1 are the most numerous and best studied among the others (Vignais & Billoud, 2007). They are attached to the membrane and connected to the electron transport chain. These membrane-bound uptake [NiFe]-hydrogenases are trimeric enzymes. They typically have an extra component known as *b*-type cytochrome for electron transfer from H_2 to the quinone pool of electron transport. This is linked to a chemiosmotic mechanism for energy conservation.

The "standard" [NiFe]-hydrogenases in Group 1, are reversibly inactivated by O_2-oxidation producing two inactive forms, Ni-A and Ni-B. A dioxygen species was reported to exist between two metals of active site in Ni-A which makes [NiFe]-hydrogenase requires a prolonged reactivation time, whereas monoxygen ligand takes place in Ni-B which can be immediately reactivated upon reduction with H_2 (Ogata *et al.*, 2009).

Generally, the standard [NiFe]-hydrogenases do not display the catalytic activity even in the presence of a trace amount of O_2 (Lubitz *et al*., 2014).

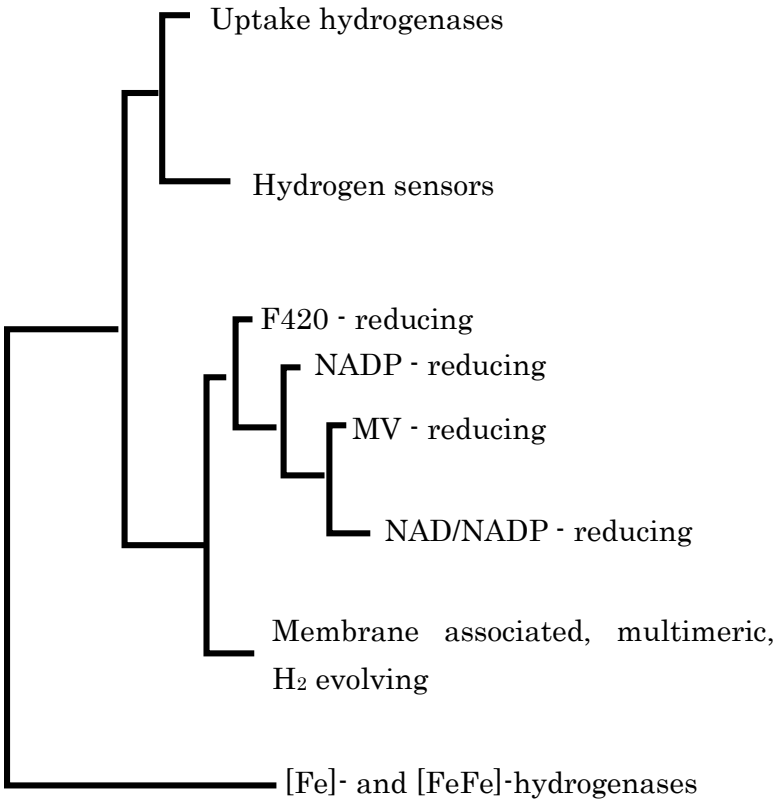

Figure 1. Schematic representation of the phylogenetic tree of [NiFe]-hydrogenases based on the complete sequences of the small and the large subunits originally established by Vignais *et al*. (2001).

The standard [NiFe]-hydrogenases are mainly composed of two subunits, called as large and small subunits (Figure 2). The small subunit contains three Fe-S clusters forming the electron transport chain. They are called proximal [4Fe-4S], medial [3Fe-4S], and distal [4Fe-4S] clusters based on their distance from the Ni-Fe active site. The small subunit has a molecular weight of typically ~29 kDa. An extended C-terminal region is often present in MBHs, which is considered to be an alpha-helical transmembrane anchor; it attaches to the physiological partner cytochrome *b*. In the large subunit (typically ~63 kDa), two metal centers are located: the Ni-Fe active site and another single metal, Mg^{2+} at the C-terminus.

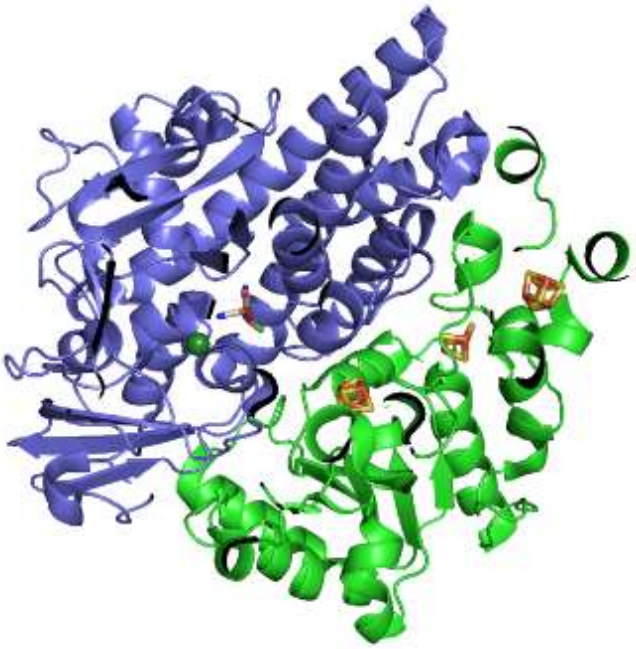

Figure 2. Ribbon representative of the overall structure of the standard [NiFe]-hydrogenase from *D.v* Miyazaki F. Large subunit and small subunit are depicted by blue and green color, respectively. The Ni-Fe active site and three Fe-S clusters are shown as stick representation in large subunit and small subunit, respectively. Green sphere is an additional metal of Mg^{2+} coordinated at C-terminus of the large subunit. Based on their distance to the Ni-Fe active site, each of the Fe-S cluster is called as a proximal [4Fe-4S], medial [3Fe-4S], and distal [4Fe-4S] clusters.

Apart from the well-studied standard [NiFe]-hydrogenases, some MBHs, however, have been found to be tolerant to O_2. MBHs in Group 1 form only Ni-B after exposure to O_2 and rapidly reactivated by H_2 to show the catalytic activity at ambient O_2 concentration (Cracknell *et al*., 2009; Pandelia *et al*., 2011). Overall structure of O_2-tolerant MBHs was found almost similar to those of the standard [NiFe]-hydrogenases except the proximal cluster. Crystal structures of O_2-tolerant MBHs revealed that they do not have a normal proximal [4Fe-4S]-4Cys cluster, but have a unique [4Fe-3S]-6Cys cluster (Shomura *et al*., 2011, Fristch *et al*., 2011) (Figure 3). In contrast to the standard [NiFe]-hydrogenases, two additional cysteine residues exist in the amino acid sequence in the small subunit of the O_2-tolerant MBH enable it to coordinate the unique [4Fe-

3S] cluster. From electrochemical and spectroscopic experiments (Goris *et al.*, 2011, Pandelia *et al.*, 2011), it has been proposed that the mechanism underlying the O_2-tolerance of MBH from *Hydrogenovibrio marinus* (MBH-mar) involves the ability of the [4Fe-3S]-6Cys cluster to donate additional electrons to the Ni-Fe active site, which is synchronized with a change in its conformation, when the enzyme is exposed to O_2 (Shomura *et al.*, 2011).

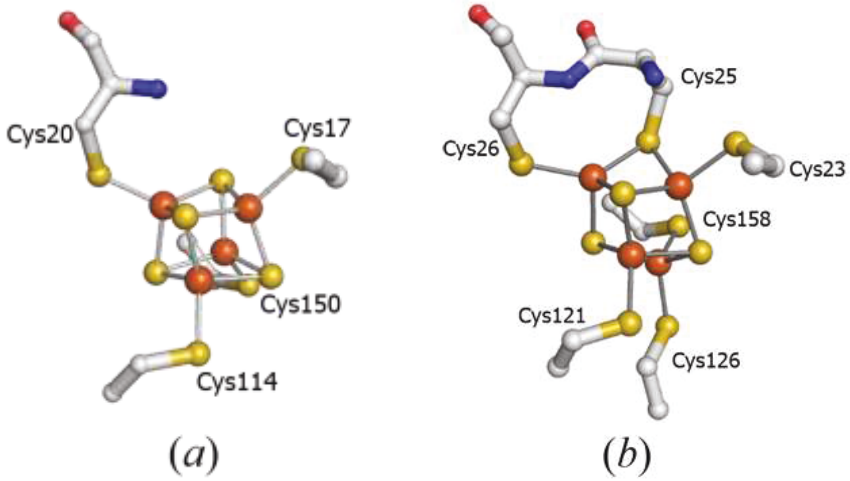

Figure 3. Proximal Fe-S cluster from (*a*) standard hydrogenase from *D.v.* Miyazaki F and (*b*) O_2-tolerant from *H. marinus* (MBH-mar). Two cysteines residues (Cys25 and Cys126) coordinated proximal [4Fe-3S] cluster of MBH-mar are highly conserved among O_2-tolerant [NiFe]-hydrogenase.

1.3 [NiFe]- hydrogenase from *Citrobacter* sp. S-77

Citrobacter sp. S-77 is a new strain from genus of *Citrobacter* which was isolated from a tepid spring (21 °C) in Aso-Kuju National Park, Oita, Japan. The [NiFe]-hydrogenase isolated from *Citrobacter* sp. S-77 was firstly identified as a heterodimeric hydrogenase. Pairwise sequence alignments (Table 1) and phylogenetic analysis (Figure 4) with other hydrogenases, showed that the heterodimeric hydrogenase from *Citrobacter* sp. S-77 is a dimeric hydrogenase unit of the Hyd-2 type [NiFe]-hydrogenase (Eguchi *et al.*, 2012). Hereafter, *Citrobacter* sp. S-77 is referred as HYD2-s77. Hyd-2 type enzymes have been reported to be sensitive to O_2 and can be reactivated by a prolonged incubation with H_2 after inactivation by O_2, like standard enzymes (Lukey *et al.*, 2010).

Biochemical studies of HYD2-s77 showed a high O_2 stability and strong specific activity of 661 U/mg (Eguchi *et al*., 2012) for H_2-oxidation at pH=7, which is a comparative to the values of 566 U/mg for the standard [NiFe]-hydrogenase from *D.v.* Miyazaki F (STD-dvm) (Yagi *et al*., 1978). Unlike O_2-sensitive hydrogenases, which usually show a significant decline of specific activity and inability of the catalytic H_2-oxidation even in the presence of a trace of O_2, oxidized HYD2-s77 can quickly restore its original activity within 90 s, even after the enzyme is exposed to a 100% pure O_2 atmosphere for 1 h (Eguchi *et al*., 2012). HYD2-s77 has a 637 times higher mass activity than Pt at 50 mV in a hydrogen half-cell. Furthermore, unlike Pt, it can be recovered 100% after poisoning by carbon monoxide (Matsumoto *et al*., 2014). These data showed that HYD2-s77 also has a remarkable O_2-stability and therefore has many advantages as an efficient H_2-activating biocatalyst in future hydrogenase technologies.

Table 1. Pairwise sequence alignment of *Citrobacter* sp. S-77 [NiFe]-hydrogenase with other hydrogenases. It has highest similarity to *E. coli* Hyd-2.

Species	Pairwise sequence alignment of heterodimeric part	Amino acid in large subunit	Amino acid in small subunit
H. marinus Hyd-1	41	611	361
R. eutropha Hyd-1	43	618	360
E. coli Hyd-1	40	597	372
E. coli Hyd-2	96	567	372
D. gigas	42	361	291
D. vulgaris Miyazaki F	43	360	317
Citrobacter sp. S-77	-	567	372

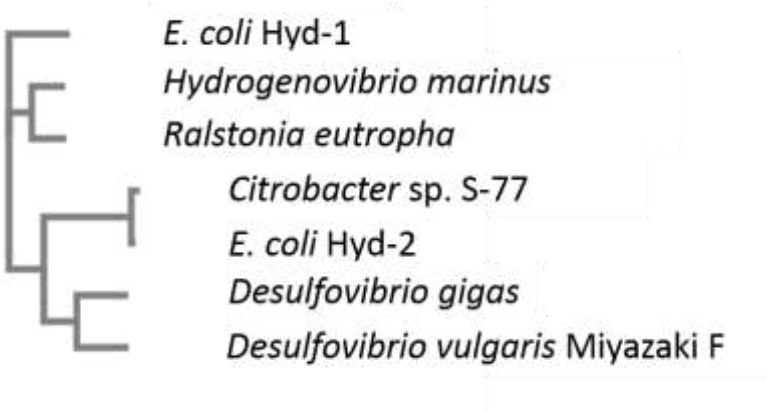

Figure 4. Phylogenetic analysis of *Citrobacter* sp. S-77 with other hydrogenases. *Citrobacter* sp.S-77 falls into one group together with *E. coli* Hyd-2.

1.4 Application of hydrogenases

Hydrogenases catalyze the cleavage and production of H_2 and have been purified and characterized from various microorganisms. Since the first crystal structure was reported by Volbeda *et al*., (1995), hydrogenases and their inspired chemical catalyst are of interest in many areas of biological and technological applications. Firstly, dihydrogen is well known for its potential as a clean energy carrier in fuel cells. Industrial catalysts for this process utilize noble metals like platinum or palladium. As a matter of fact, nature utilizes earth-abundant base metals, such as nickel and iron for this purpose. Since hydrogenase catalyzes the oxidation of H_2 to protons, and coupling this reaction to an enzyme-catalyzed reduction, such that O_2 to O^{2-}, this process will only produce water and electricity as the byproducts (Chenevier *et al*., 2013). Large scale fermentative and/or phototropic hydrogen generation is also often discussed, as model systems or organisms that contain hydrogenases directly coupled to photosystem I and II could be engineered for photoinduced hydrogen production (Mertens & Liese, 2004).

1.5 Objectives of study

Most [NiFe]-hydrogenases are highly sensitive to O_2, which causes loss of catalytic activity after oxidation by air (Vignais and Billoid, 2007). However, some [NiFe]-hydrogenases purified from H_2-oxidizing bacteria show unusual high O_2-tolerance,

which exhibit catalytic activity in the presence of the ambient O_2-concentration. This characteristic has opened up a new possibility to implement of actual enzymes into biotechnological fuel cells. From biochemical properties of HYD2-s77, it also showed that this enzyme has potential of an O_2-stable hydrogenase. Hyd-2 type enzymes might be of great interest, if we can elucidate the molecular mechanism for the O_2-stability and or O_2-tolerance of HYD2-s77.

Therefore aim of this study is to investigate structural and functional relationship of HYD2-s77 in order to provide detail mechanisms of this new candidate O_2-tolerant [NiFe]-hydrogenase. Understanding the molecular basis behind this O_2-tolerance, and what processes are involved in enzyme biosynthesis are therefore important research objectives. This will be achieved by performing purification, crystallization, X-ray diffraction, and structural elucidation of HYD2-s77 in different redox states. We believe this information will provide breakthrough for the chemical development of hydrogenase-based biofuel cells.

In this dissertation, purification, crystallization, O_2-tolerant property and preliminary crystallographic study are documented.

2.0 Materials and methods

2.1 Preparation of media, buffers and solutions

The composition of media, buffers and standard solution used in this study are listed in Table 2.

Table 2. List of preparation of media, buffers and solutions.

Media/ Buffers/ Solutions (g/L)	Composition
Yeast extract culture medium	Yeast extract (3.0 g), Polypeptone (3.0 g), $(NH_4)_2SO_4$ (3.0 g), $MgSO_4$. $7H_2O$ (0.5 g), K_2HPO_4 (2.0 g), KH_2PO_4 (1.0 g), $Na_2S_2O_3.5H_2O$ (2.0 g), Ammonium ferric citrate (0.2 g) $CaCl_2$ (0.1 g). Prepared media are autoclaved at 121°C for 30 min.
10 mM MOPS pH 7.0	MOPS (2.1 g), adjust pH to 7.0 with concentrated NaOH
10 mM MOPS pH 7.0, 1 M NaCl	MOPS (2.1 g), NaCl (58.44 g), adjust pH to 7.0 with concentrated NaOH
10 mM MOPS pH 7.0, 0.2 M $(NH_4)_3$ SO_4	MOPS (2.1 g), $(NH_4)_3$ SO_4 (26.4 g), adjust pH to 7.0 with concentrated NaOH
20 mM MOPS pH 7.0, 1.0 mM benzyl viologen (1,1'-dibenzyl-4,4'-bipyridinium dichloride), 1.0 mM TTC (2,3,5-triphenyl-2H-tetrazolium chloride)	MOPS (4.19 g), Benzyl viologen (0.41 g), TTC (0.36 g)
10X Tris Glycine electrophoresis buffer for SDS-PAGE	Tris base (30.3 g), glycine (144.0 g), SDS (10.0 g)
10X Tris Glycine electrophoresis buffer for NATIVE-PAGE	Tris base (30.3 g), glycine (144.0 g)
5X sample buffer (SDS reducing buffer)	2 M Tris-HCl (pH 6.8), SDS (10.0 g), glycerol (30.0 mL), bromophenol blue (trace 0.02%), distilled water

2.2 Cultivation of *Citrobacter* sp. S-77

Bacterial stock of *Citrobacter* sp. S-77 was kept in 50% v/v glycerol stock at 193 K. Prior to main media cultivation, 2 ml of bacterial stock was transferred to 200 ml culture

media for preculture. The bacterium was precultured under aerobic condition in yeast extract medium at pH 6.8 to 7.0 at 303 K for 24 h in 500 ml Schott Duran bottles. Main culture was prepared by transferring 50 ml volume of the preculture to each four bottles of 10 L Nalgene Carboy (Thermo Fisher Scientific, USA) containing 8 L autoclaved culture medium. Media preparation was shown in Table 2. The culture media was incubated for 72 hours at 303 K before harvesting at 10,630 × *g* for 10 minutes, at 277 K. About 65.0 g to 70.0 g bacterial cells were obtained from 32 L bacterial culture. The collected cells were frozen by using liquid nitrogen prior to storage at 193 K.

2.3 Membrane cell solubilization and purification of HYD2-s77

The obtained cells (65.0 g) were suspended in 20 mM MOPS pH 7.0 then disrupted by ultrasonication (Qsonica Sonicator Q700, Thermo Fisher Scientific, USA). The lysate was ultracentrifuged (Himac CP 70 MX, Hitachi, Japan) at 142,200 × *g* for 60 min at 277 K. The collected membrane fractions were suspended in 20 mM MOPS pH 7.0, 1.0 mM DTT and solubilized by adding the same volume of the buffer containing nonionic detergent of 2.0 % Triton X-100. After adding the detergent, the suspended solution was slowly stirred overnight at 277 K in an anaerobic chamber (Model B, Coy Laboratory Products, Grass Lake, Michigan, USA) under an atmosphere of 98% N_2 and 2% H_2. The extract was then ultracentrifuged at 142,200 × *g* for 60 min. For the sample without trypsin digestion, the supernatant was directly loaded onto the first purification step. Whereas the supernatant was treated with a final concentration of 0.1 mg/mL of trypsin for 60 min at 37 °C prior to first column chromatography for the sample treated with trypsin. Subsequently, all same purification procedures was applied for both protein samples with and without trypsin treatment.

All purification procedures were carried out at room temperature under strictly anaerobic condition using the anaerobic chamber. All buffers were filtered and were repeatedly degassed in the anaerobic chamber. The purification columns were equilibrated with degassed buffer prior to use. Liquid chromatography was performed using an AKTAprime Plus (GE Healthcare, Little Chalfont, UK). Solubilized membrane proteins were firstly loaded onto an initial anion exchange column of DEAE

Sepharose FF (2.6 x 12 cm in XK26/20 column, GE Healthcare, Little Chalfont, UK) equilibrated with 10 mM MOPS pH 7.0, 0.03% Triton X-100, 1.0 mM DTT. The hydrogenase was eluted at approximately 250 mM NaCl from a linear concentration gradient of NaCl (0-0.5 M in 4 column volumes) in the same buffer solution (flow rate: 5.0 ml/min). The fractions that showed significant activity were collected and pooled for the next step. The pooled fractions were further purified by using a second application of anion exchange chromatography, with a HiTrap Q HP (5 ml; GE Healthcare, Little Chalfont, UK) equilibrated with 10 mM MOPS pH 7.0, 1.0 mM DTT without detergent. The hydrogenase was eluted at approximately 200 mM NaCl from a linear concentration gradient of NaCl (0-0.4 M in 20 column volumes) in the same buffer solution (flow rate: 4.0 ml/min). The final step used was hydrophobic chromatography. The pooled hydrogenase fractions were mixed with the same volume of 10 mM MOPS pH 7.0, 1.0 mM DTT containing 0.4 M ammonium sulfate and applied onto a HiTrap Phenyl HP (5 ml; GE Healthcare, Little Chalfont, UK). The column was pre-equilibrated with 0.2 M ammonium sulfate in 10 mM MOPS pH 7.0, 1.0 mM DTT. The protein was eluted at approximately 80 mM ammonium sulfate from a linear concentration gradient of ammonium sulfate (0.2-0.0 M in 10 column volumes). Fractions with high purity was pooled together and finally dialysis against 10 mM MOPS pH 7.0, 0.2 M NaCl prior to protein crystallization. Dialyzed protein solution was concentrated using a Vivaspin (5,000 Da molecular weight cutoff, GE Healthcare, Little Chalfont, UK) up to 30 mg/ml.

2.4 NATIVE-PAGE activity staining and SDS-PAGE analysis

After running NATIVE-PAGE, the polyacrylamide gel (8%) was soaked in 50 ml of 20 mM MOPS pH 7.0 containing 1.0 mM benzyl viologen (1,1'-dibenzyl-4,4'-bipyridinium dichloride; Sigma-Aldrich; Seelze, Germany), 1.0 mM TTC (2,3,5-triphenyl-2H-tetrazolium chloride; BD, Sparks, Maryland), and incubated at 303 K with H_2 bubbling (50 ml/min, 0.1 MPa) for 10 min. The migrated active hydrogenase in the gel displayed the red band caused by reduction of TTC to TPF (1,3,5-triphenylformazan) due to the H_2-dependent catalytic reaction by the enzyme. The hydrogenase activity in each fraction after chromatography was checked by NATIVE-

PAGE activity staining, and active fractions were pooled and applied on the next column. In final step hydrophobic chromatography, the elution peak corresponding to the target protein was assessed by 13% acrylamide SDS-PAGE gel. Ingredients used for NATIVE-PAGE and SDS-PAGE are as in Table 3 and 4, respectively.

Table 3. Ingredients used for NATIVE polyacrylamide gel.

Percent Gel	Separating (8.0 %)	Stacking (5.0 %)
dH_2O	2.14 ml	915 µl
40% Acrylamide	800 µl	1.5 ml
4× Wide Range gel preparation buffer (Nacalai Tesque)	1.00 ml	375 µl
10% (w/v) SDS	40 µl	15 µl
10% (w/v) Ammonium persulfate	10 µl	4 µl
TEMED	3 µl	3 µl

Table 4. Ingredients used for SDS polyacrylamide gel.

Percent Gel	Separating (13.0 %)	Stacking (5.0 %)
dH_2O	1.62 ml	915 µl
40% Acrylamide	1.32 ml	1.5 ml
1.5 M Tris-HCl pH 8.8	1.00 ml	-
0.5 M Tris-HCl pH 6.8	-	375 µl
10% (w/v) SDS	40 µl	15 µl
10% (w/v) Ammonium persulfate	10 µl	4 µl
TEMED	3 µl	3 µl

2.5 Quantitative enzyme assay and protein concentration

The quantitative enzyme assay for each purification step was performed according to the protocols described in the previous paper (Eguchi *et al.*, 2012). Total protein concentration of the sample from each purification step were determined using DC Protein Assay (Bio-Rad, California, USA).

2.6 Oxygen tolerance property

A solution of 25 mM potassium phosphate (KP) buffer (pH 7.0) with 5% (w/v) TTC was pre-saturated with Ar bubbling, and then saturated with H_2. A solution of hydrogenases (HYD2-s77, MBH-mar and STD-dvm) in 25 mM KP buffer was pre-activated by H_2 bubbling for 30 min at a flow rate of 50 ml/min. Monitoring of the enzymatic reaction was initiated by addition of 300 μl of TTC buffer solution to 2700 μl of a reaction mixture with 3.3×10^{-3} μM of each enzyme in a glass cuvette with a rubber stopper and aluminum cap (path length: 10 mm) at 310 K. In order to determine the O_2 tolerance of the H_2-consumption activity, TTC with O_2 and TTC saturated with H_2 buffer solutions were mixed in various ratios, and introduced into the reaction cuvette. The TTC buffer solution containing O_2 was prepared under an aerobic condition. This solution is air-equilibrated and suppose to contain 210 μM of O_2 at ambient temperature and pressure (Hocking M.B., 1998). H_2-consumption activity was monitored and estimated by the increase of the absorption at 546 nm due to the H_2-dependent reduction of TTC using a spectrophotometer. The index of O_2 tolerance was defined as the 100-fold inverse of the reactivation time (minute) of the enzyme when the H_2-consumption catalytic reaction rate, the slope ($\Delta Abs/\Delta t$) of the tangent line of the H_2-consumption activity curves as shown in the results, reached its maximum value with each amount of O_2. For comparison, other [NiFe]-hydrogenase, MBH-mar and STD-dvm, were also measured for their H_2-consumption activity using TTC assay. The protein samples used were prepared according to the methods reported previously for MBH-mar (Yoon *et al.*, 2011) and STD-dvm (Higuchi *et al.*, 1987).

2.7 Crystallization

Crystallization condition was screened by using many commercial kits; JBScreen PEG/Salt HTS, Pi-PEG Screen, and JBScreen Classic HTS1 (Jena Biosciences, Jena, Germany). The crystallization plates from each of the formulation kit were incubated at 277 K and 283 K. HYD2-s77 was crystallized by the sitting drop vapor diffusion method in 96 wells MRC 2-well crystallization plate (Hampton Research, Aliso Viejo, CA, USA). A few optimization steps, including the concentration of the protein and precipitants, were performed in protein crystallization in order to get best crystals for

X-ray diffraction measurement. For optimization, the concentration for the protein sample was optimized. Crystallization drop size was 1.0 μl (0.5 μl protein + 0.5 μl reservoir solution).

For protein sample without trypsin treatment, different protein concentrations (9, 11, 13 mg/ml of the enzyme) were screened against one condition of precipitant; 18% w/v PEG 10,000, 20% (w/v) glycerol, 0.1 M NaCl, 0.1 M Tris-HCl, pH 8.5. Best combination of protein and precipitant concentration were repeated for reproducibility. Due to higher yield of sample with trypsin treatment, after final chromatography, optimization could be done for many protein concentrations (9, 11, 13, 15 and 17 mg/ml of the enzyme). At first, by using the same concentration of 11 mg/ml from previous attempt, different condition of PEG 10,000 and NaCl were screened. 2D grid screen was used as the method for optimization. The concentration of PEG was screened against the concentration of NaCl as shown in the Figure 5. Good shape but smaller crystals was obtained from 19% PEG 10,000, 20% (w/v) glycerol, 0.1 M NaCl, 0.1 M Tris-HCl, pH 8.5. Therefore, another optimization of protein concentration and NaCl was done with 19% (w/v) of PEG10,000 (Figure 6).

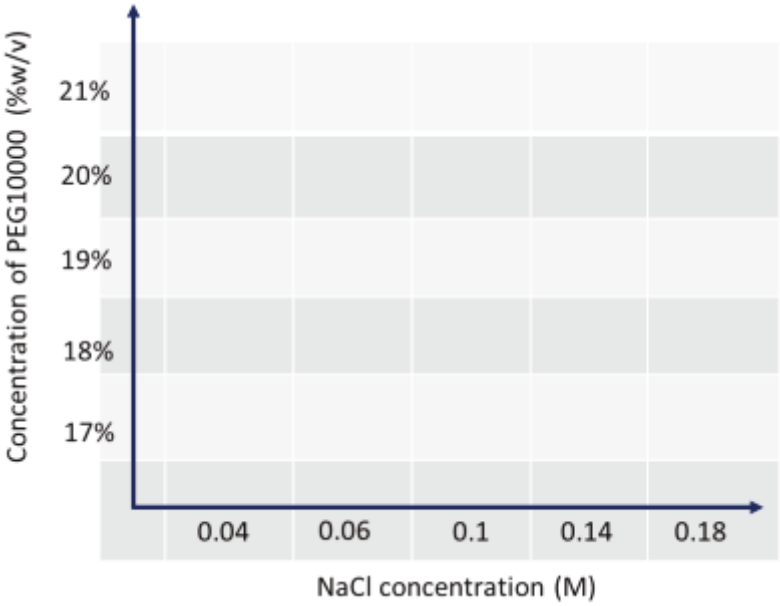

Figure 5. 2D grid screen diagram used for optimization of the concentration of PEG10,000 and NaCl in crystallization formulation. The concentration of PEG 10,000 (17-21 % (w/v)) was screened against that of NaCl (0.04-0.18 M). Protein was fixed to 11 mg/ml.

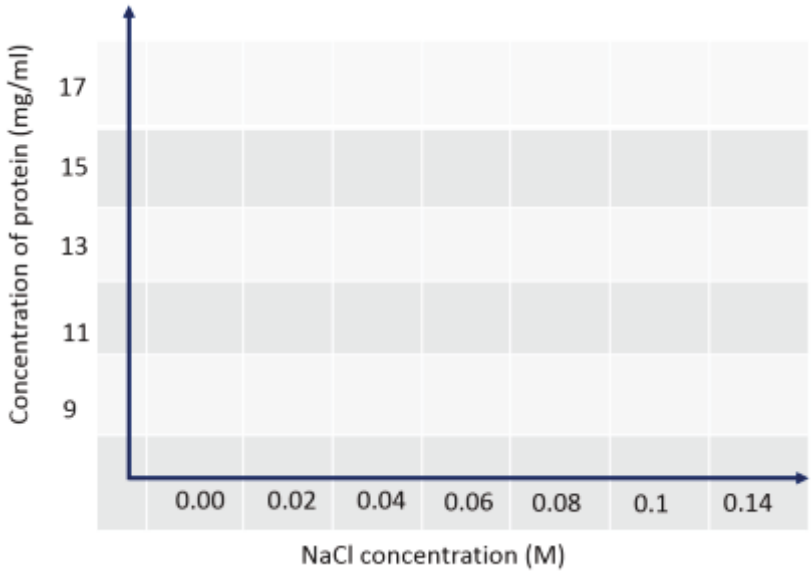

Figure 6. 2D grid screen diagram used for optimization of the concentration of protein and NaCl in crystallization formulation. The concentration of the protein (9-17 mg/ml) was screened against that of NaCl (0.00-0.14 M). PEG10,000 was fixed to 19% (w/v).

Protein crystallization was performed at 10°C. After optimization, the concentrations for protein with and without trypsin digestion treatment used were 15 mg/ml and 11 mg/ml with combination of 19% PEG 10,000 and 18% PEG 10,000, respectively.

2.8 Data collection and processing

The X-ray diffraction experiment was carried out at the BL44XU beamline of SPring-8 using an MX300HE detector. The crystals were soaked in a cryoprotectant solution (reservoir solution) and mounted in nylon loops (Hampton Research, Aliso Viejo, CA, USA), and then flash cooled in a nitrogen stream at 100 K. The X-ray wavelength employed for data collection was 0.9000 Å. The crystal-to-detector distance, rotation range, exposure time for each frames, and total number of frames for samples not treated with trypsin were 190 mm, 1.0 ˚, 1.0 s and 180, respectively, whereas those for sample subjected to trypsin treatment were 160 mm, 0.5 ˚, 0.5 s, and 360, respectively. Details on data collection and processing are summarized in Table 7. Diffraction images were indexed using iMOSFLM from CCP4 program suite (Collaborative Computational Project, Number 4, 1994). Each data set was merged and scaled by using SCALA (Evans, P., 2006).

3.0 Results

3.1 Purification of HYD2-s77

3.1.1 Purification without trypsin treatment

In the first chromatography DEAF FF chromatography, HYD2-s77 was eluted around 0.25 M NaCl (Figure 7). About 50 ml of HYD2-s77 from five fractions with hydrogenase activity were pooled for the second step chromatography.

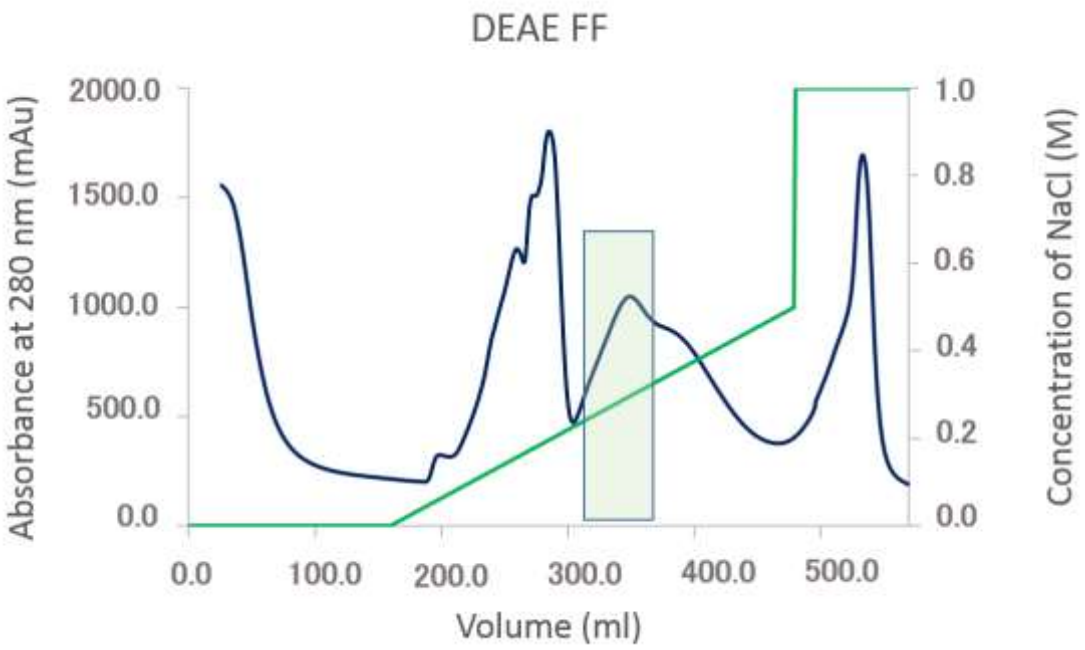

Figure 7. Elution profile of HYD2-s77 on DEAE FF chromatography. The protein absorption pattern monitored at 280 nm and NaCl linear gradient are shown in blue and green lines, respectively. The pooled five fractions with hydrogenase activity are enclosed in green box.

The pooled fractions from the first step chromatography were applied on the HiTrapQ HP column. The target hydrogenase was eluted approximately at 0.2 M NaCl (Figure 8). About 15 ml of HYD2-s77 from three fractions were pooled for the third step chromatography.

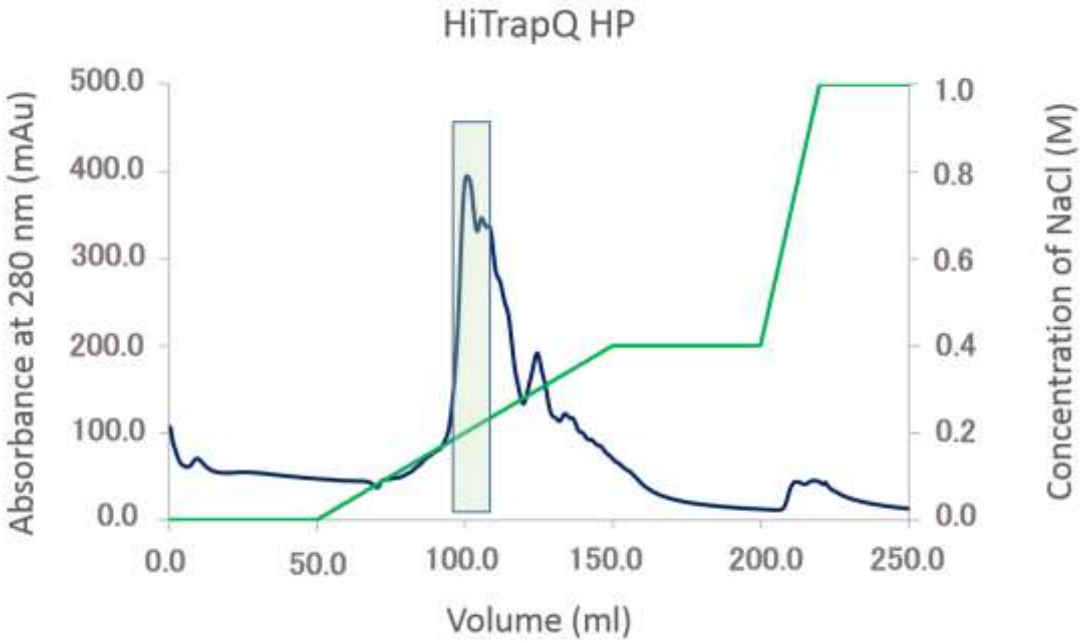

Figure 8. Elution profile of HYD2-s77 on HiTrap Q HP anion exchange chromatography. The protein absorption pattern monitored at 280 nm and NaCl linear gradient are shown in blue and green lines, respectively. The pooled three fractions with hydrogenase activity are enclosed in green box.

Third step separation was carried out based on hydrophobic interaction chromatography. The pooled fractions from the previous step were further applied on HiTrap Phenyl HP column. Fractions of the target hydrogenase were eluted at 0.03-0.05 M ammonium sulfate (Figure 9) and were analyzed by using NATIVE-PAGE and SDS-PAGE (Figure 10(*c*) and (*d*)). Fractions showed red band on NATIVE-PAGE and highly purified fractions based on SDS-PAGE analysis were pooled for dialysis against 10 mM MOPS pH 7.0 containing 0.2 M NaCl.

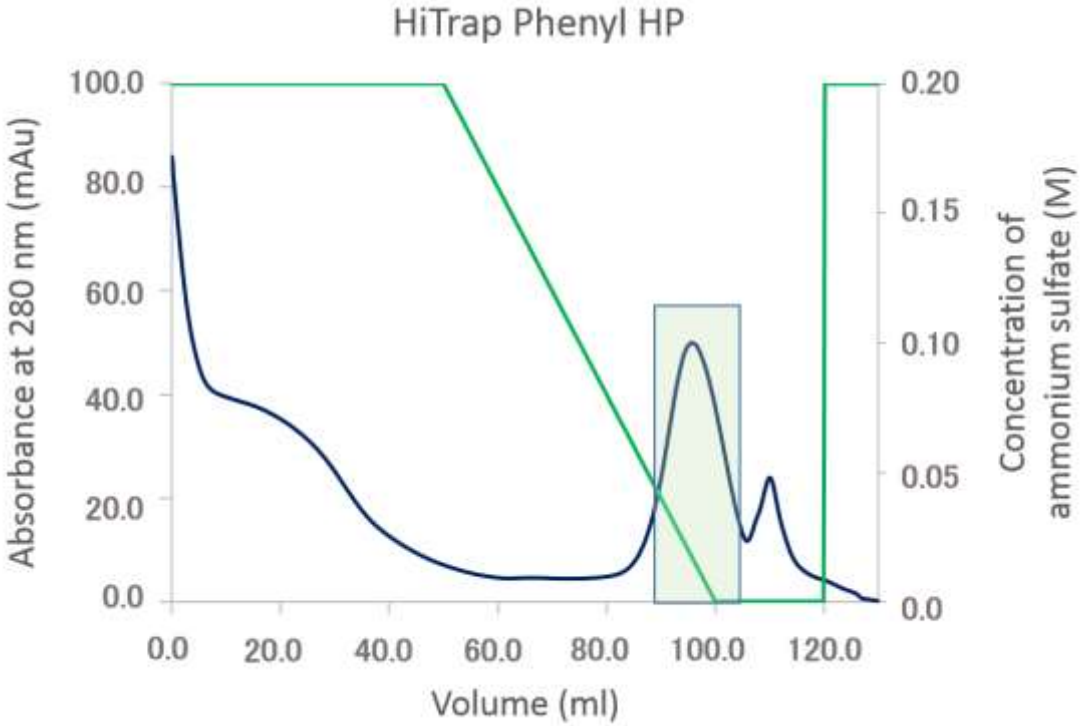

Figure 9. Elution profile of HYD2-s77 on HiTrap Phenyl HP chromatography. The protein absorption pattern monitored at 280 nm and $(NH_4)_2SO_4$ linear gradient are shown in blue and green lines, respectively. The pooled eight fractions with hydrogenase activity are enclosed in green box.

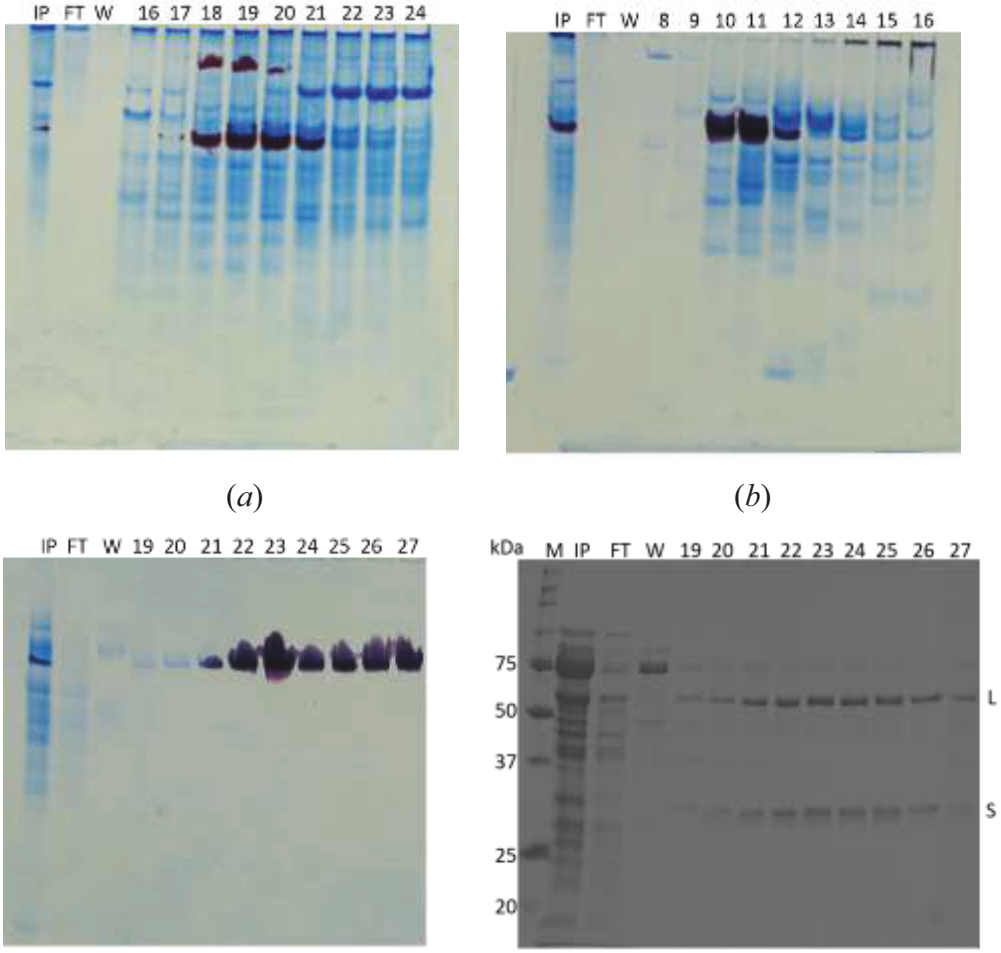

Figure 10. NATIVE-PAGE activity staining and SDS-PAGE analysis after purification of HYD2-s77. (*a*), (*b*), (*c*) are NATIVE-PAGE activity staining results for the fractions after DEAE FF, HiTrap Q HP and HiTrap Phenyl HP, respectively. (*d*) SDS-PAGE analysis after HiTrap Phenyl HP chromatography. L and S indicate the protein bands for the large and small subunits, respectively. M, IP, FT, and W indicate the "Standard protein marker (in kDa)", "Input", "Flow through" and "Wash" fractions, respectively for each chromatography.

3.1.2 Purification with trypsin treatment

The supernatant after final centrifugation was treated with 0.1 mg/ml trypsin at 37°C for 1 h and directly loaded onto the first column of DEAE FF chromatography. The target hydrogenase was eluted at approximately 0.25 M NaCl (Figure 12). Fractions of target hydrogenase were checked by using NATIVE-PAGE activity staining (Figure 14 (*a*)).

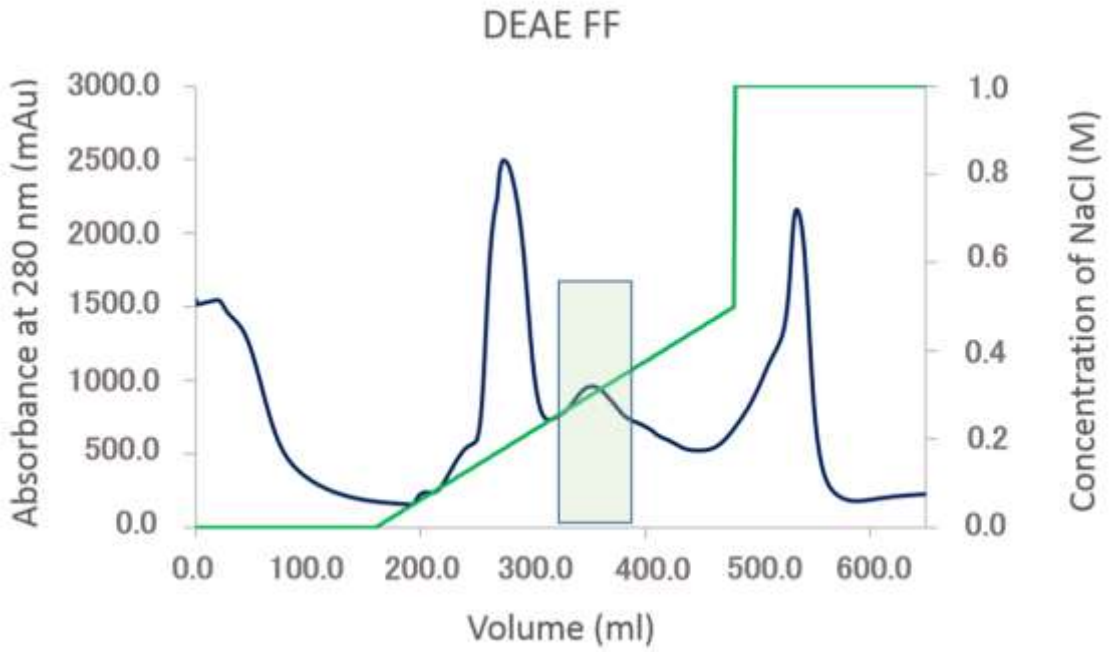

Figure 11. Elution profile of HYD2-s77 on DEAE FF chromatography. The protein absorption pattern monitored at 280 nm and NaCl linear gradient are shown in blue and green lines, respectively. The pooled fractions with hydrogenase activity are enclosed in green box.

The pooled fractions after first step chromatography were applied on the HiTrapQ HP column. The target hydrogenase was eluted approximately at 0.2-0.25 M NaCl (Figure 12). About 30 ml of HYD2-s77 from six fractions was pooled for the third step chromatography (Figure 14(*b*)).

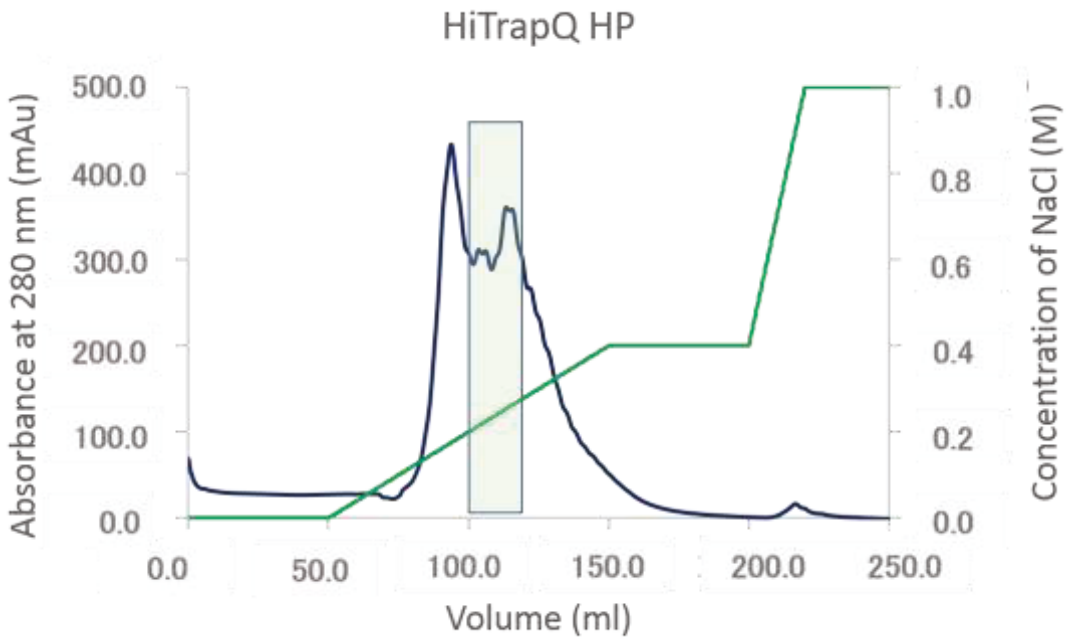

Figure 12. Elution profile of HYD2-s77 on HiTrap Q HP anion exchange chromatography. The protein absorption pattern monitored at 280 nm and NaCl linear gradient are shown in blue and green lines, respectively. The pooled six fractions with hydrogenase activity are enclosed in green box.

The pooled fractions from the previous step were further applied on HiTrap Phenyl HP column. The fractions of the target hydrogenase were eluted at 0.08-0.05 M ammonium sulfate (Figure 13) and were analyzed by using NATIVE-PAGE and SDS-PAGE (Figure 14(*c*) and (*d*)). Fractions showed red band on NATIVE-PAGE and highly purified fractions based on SDS-PAGE analysis were pooled for dialysis against 10 mM MOPS pH 7.0 containing 0.2 M NaCl.

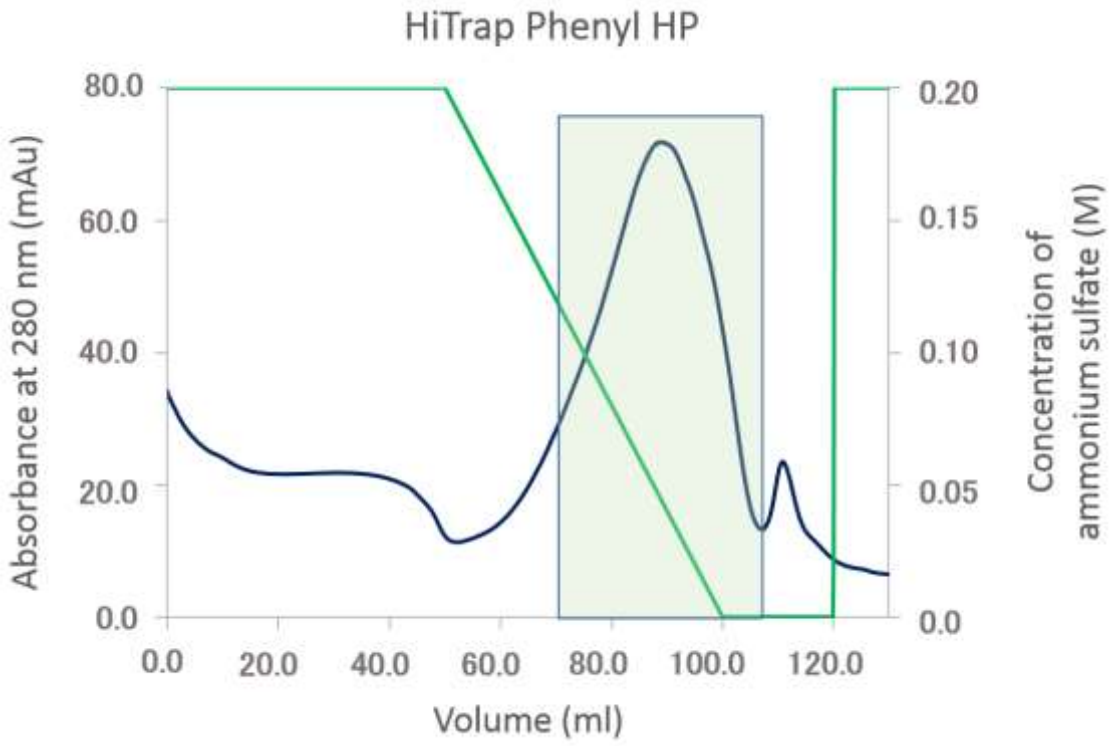

Figure 13. Elution profile of HYD2-s77 on HiTrap Phenyl HP chromatography. The protein absorption pattern monitored at 280 nm and $(NH_4)_2SO_4$ linear gradient are shown in blue and green lines, respectively. The pooled fifteen fractions with hydrogenase activity are enclosed in green box.

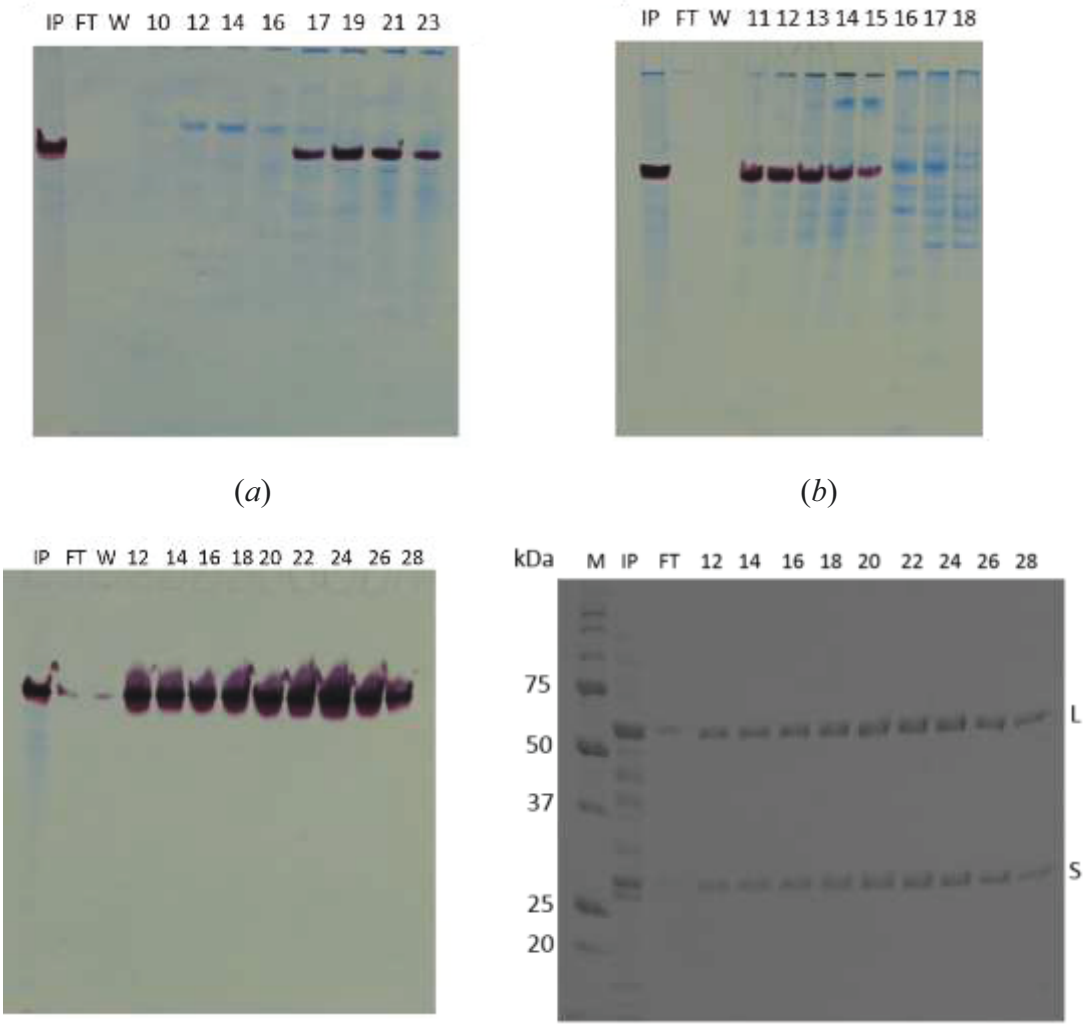

Figure 14. NATIVE-PAGE activity staining and SDS-PAGE analysis after purification of HYD2-s77. (*a*), (*b*), (*c*) are NATIVE-PAGE activity staining results for the fractions after DEAE FF, HiTrap Q HP and HiTrap Phenyl HP, respectively. (*d*) SDS-PAGE analysis after HiTrap Phenyl HP chromatography. L and S indicate the protein bands for the large and small subunits, respectively. M, IP, FT, and W indicate the "Standard protein marker (in kDa)", "Input", "Flow through" and "Wash" fractions, respectively for each chromatography.

Efficiency of both purification steps were compared in Table 5. The purity of HYD2-s77 was improved by applying trypsin in purification step. Recovery was increased for about 70% compared to the purification without trypsin. These results clearly show that the trypsin treatment was effective for getting a sufficient amount of the protein sample in high purity for further crystallization screenings.

Table 5. Purification of Hyd-2 type [NiFe]-hydrogenase from *Citrobacter* sp. S-77. Starting bacterial cell pellet was 65.0 g for both purification procedures without and with trypsin treatment.

Purification step	Activity (U)		Protein (mg)		Specific activity (U/mg)		Recovery (%)		Purity (fold)	
Trypsin treatment (0.1 mg/ml)	-	+	-	+	-	+	-	+	-	+
Membrane	7254	6420	48109	22630	0.15	0.28	100	100	1	1
Solubilization	4903	6040	2583	678	1.90	8.91	67.6	94.1	12.7	31.8
DEAE FF	3259	5612	384	59.9	8.49	93.7	44.9	87.4	56.6	335
HiTrap Q FF	2195	3403	90.0	21.8	24.4	156	30.3	53.0	163	557
HiTrap Phenyl HP	915	3114	3.92	5.37	233	580	12.6	48.5	1553	2071

3.2 Oxygen tolerant property

By using TTC as the electron acceptor, the O_2 tolerances of three different enzymes were investigated and compared. The H_2-consumption activity of MBH-mar promptly recovered, even in the presence of a significant amount (63.0 nmol) of O_2, indicating that the enzyme retained the activity and consumed O_2 due to its catalytic reaction that produces an H_2–dependent reducing power (Figure 15(*a*)). STD-dvm, the typical standard [NiFe]-hydrogenase, showed a strong H_2-consumption activity without O_2, but the activity could not be recovered in the presence of a small amount (4.2 nmol) of O_2 (Figure 15(*b*)). HYD2-s77 showed a relatively prolonged lag time for the various O_2 concentrations compared with MBH-mar, but the activity was recovered in the presence of 63.0 nmol of O_2 (Figure 15(*c*)). The calculated O_2 tolerance indexes in the presence of 4.2, 8.4, 12.6, 31.5, and 63.0 nmol of O_2 were 120.0, 98.4, 93.8, 14.4 and 8.30 for MBH-

mar, and 46.9, 20.5, 17.1, 2.44 and 1.34 for HYD2-s77, respectively. The results presented here demonstrate that HYD2-s77 also retained catalytic activity toward H_2 consumption in the presence of some amount of O_2, suggesting that HYD2-s77, one of the Hyd2-type enzymes, has an obvious O_2 tolerance.

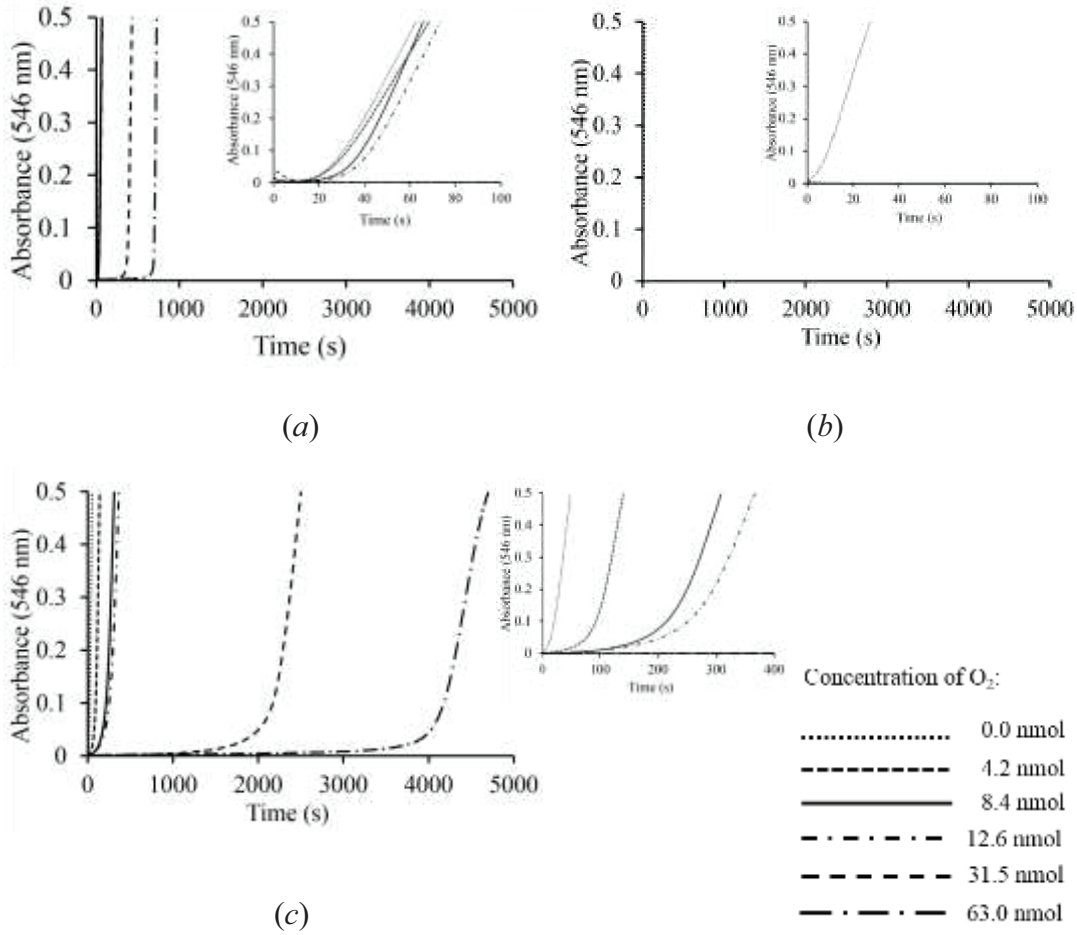

Figure 15. The effect of O_2 on the H_2-consumption activity of the purified enzymes from (a) MBH-mar, (b) STD-dvm and (c) HYD2-s77. The inset of (a) and (c) show magnification of absorbance data for MBH-mar and HYD2-s77 with 0.0 to 12.6 nmol O_2, respectively. Inset of (b) shows magnification of absorbance data for STD-dvm at 0.0 to 4.2 nmol O_2. O_2-tolerance of all hydrogenases were estimated by measuring the time of the revival of the activity without and with a certain amount of O_2-containing triphenyltetrazolium chloride. O_2-tolerance indexes in the presence of 4.2, 8.4, 12.6, 31.5 and 63.0 nmol of O_2 were calculated to be 120.0, 98.4, 93.8, 14.4 and 8.30 for MBH-mar, and 46.9, 20.5, 17.1, 2.44 and 1.34 for HYD2-s77, respectively.

3.3 Crystallization of HYD2-s77 without trypsin treatment

At early stage, the crystallization condition was screened by using sample without trypsin treatment. Two crystallization conditions gave the crystals shown in Table 6. Formulation H7 (JBScreen Classic HTS1), which gave the better crystals in shape, was chosen for further optimization.

Table 6. Screening conditions for the initial crystallization trials of HYD2-S77.

Precipitant	E7 from JBScreen PEG/ Salt HTS	H7 from JBScreen Classic HTS1
Compositions	20% (w/v) PEG 5000 MME, 0.2 M ammonium dihydrogen phosphate	18% (w/v) PEG 10,000, 20% (w/v) glycerol, 0.1 M Tris-HCl pH 8.5, 0.1 M NaCl
Protein concentration	2.8 mg/ml	4.3 mg/ml
Ratio/volume (protein : reservoir)	0.5 μL : 0.5 μL	0.5 μL : 0.5 μL
Temperature	277 K	283 K
Crystals appearance	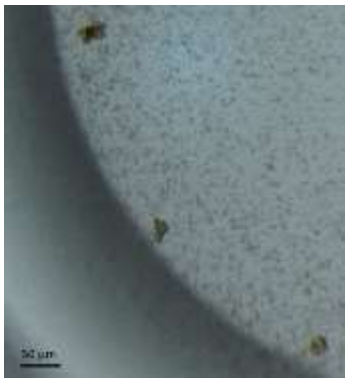 Crystals appeared after 2-3 days	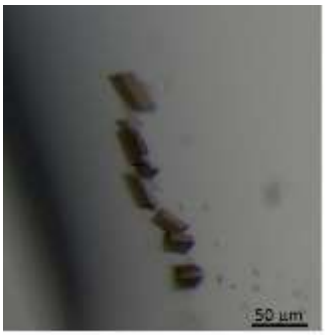 Crystals appeared after 2-3 days

3.3.1 Optimization of protein concentration

Initial screening condition was optimized by varying the protein concentration. Protein concentration was controlled by mixing different ratio protein volume to reservoir solution. Protein concentration used was 11 mg/ml. Plate-like crystals were obtained from combination of 0.4 μl protein solution to 0.6 μl reservoir at 283 K (Figure 16). Other

formulation conditions produced amorphous precipitation.

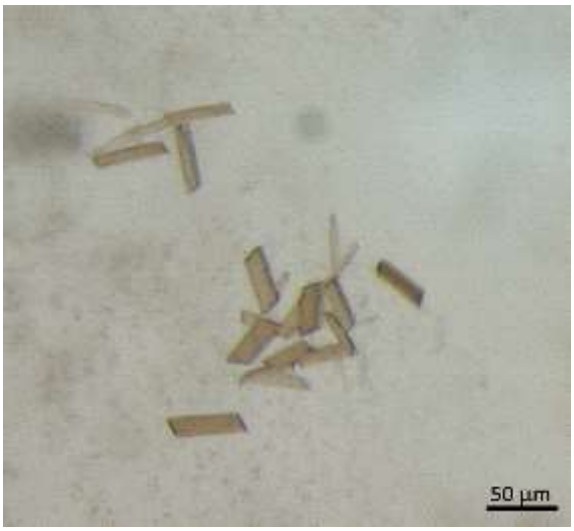

Figure 16. Crystals obtained by the optimization of the concentration of the protein.
Plate-like thin crystals were obtained by using 18% (w/v) PEG 10,000, 20% (w/v) glycerol, 0.1 M Tris-HCl pH 8.5, 0.1 M NaCl as the precipitant.

Loss of the protein sample, during the protein concentration process due to the adsorption of the protein samples to the membrane materials of a concentrator, was the crucial problem. The protein solution from the final step chromatography was dialyzed against 10 mM MOPS pH 7.0, 0.2 M NaCl. To dialyze the protein solution against 0.2 M NaCl buffer solution was found to be effective to reduce the non-specific adsorption occurred between the membrane filter material and protein sample. For further crystallization experiment, only the protein solution equilibrated with 0.2 M NaCl was applied for crystallization.

3.3.2 Optimization of precipitant

For optimization of precipitant concentration, three protein concentration of 9.0, 11.0, and 13 mg/ml protein concentration were used. Precipitant formulation which contain 15-20% (w/v) of PEG10,000 was applied in the crystallization experiments. Each of the mixture of 0.5 µl protein solution and 0.5 µl reservoir was used. Best crystals was obtained by using combination of 11 mg/ml protein with reservoir contains 18% (w/v) PEG10,000,

20% (w/v) glycerol, 0.1 M NaCl, 0.1 M Tris-HCl pH 8.5 within 2-3 days. The results of crystallization optimization are shown in Table 7.

Table 7. Score sheet for the crystallization at various concentrations of PEG10,000 and HYD2-s77

PEG 10,000 Conc. % (w/v) / Protein Conc. (mg/ml)	15	16	17	18	19	20
9.0	No crystals	No crystals	No crystals	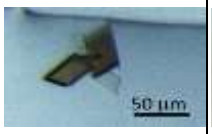		No crystals
11.0	No crystals	No crystals			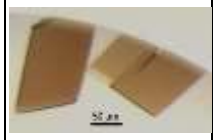	
13.0	No crystals	No crystals	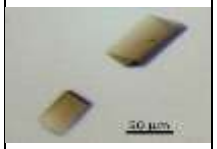			

Reproducibility of crystallization by using 18% (w/v) PEG10,000, 20% (w/v) glycerol, 0.1 M NaCl, 0.1 M Tris-HCl pH 8.5 was shown in Figure 17.

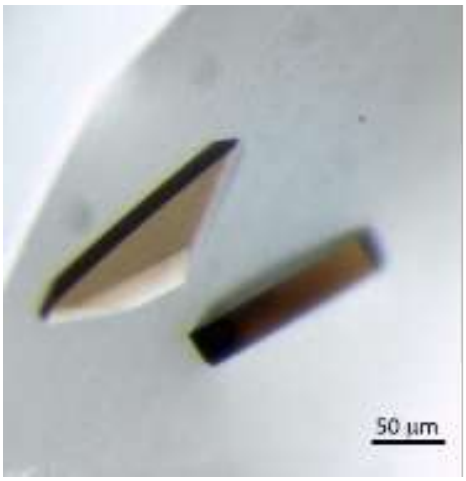

Figure 17. HYD2-s77 crystals obtained from the optimized condition. Crystals were obtained from the droplets consisting of 0.5 µl of 11 mg/ml of the protein and 0.5 µl of 18% (w/v) PEG10,000, 20% (w/v) glycerol, 0.1 M Tris-HCl pH 8.5 and 0.1 M NaCl of the reservoir solution.

3.4 Crystallization of HYD2-s77 with trypsin treatment

3.4.1 Optimization of protein and precipitant

At early stage, the crystallization for HYD2-s77 with trypsin treatment using the same condition as that without trypsin treatment was not successful. Therefore, the crystallization condition was screened and optimized for the trypsin-treated HYD2-s77 using PEG10,000 and NaCl.

The best crystals were obtained from 19% PEG 10,000 with combination of 0.1 M NaCl. The size of the obtained crystals are small even though the thickness was improved than the previous crystals without trypsin-treatment (Figure 18).

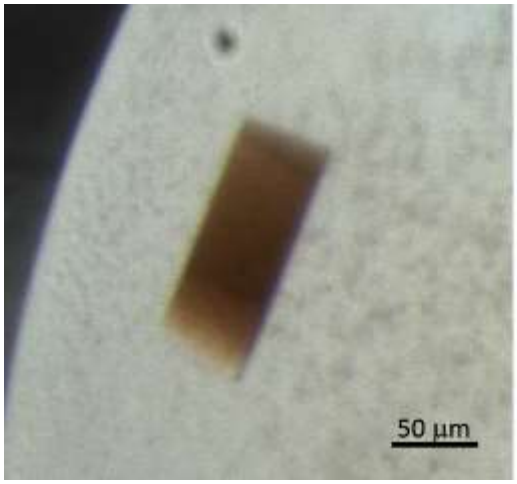

Figure 18. HYD2-s77 crystals obtained from the initial improved condition. The droplet contained 11 mg/ml of the protein and 19% (w/v) PEG10,000, 20% (w/v) glycerol, 0.1 M Tris-HCl pH 8.5 and 0.1 M NaCl as the reservoir.

By using 2D grid screen, optimization on protein concentration against NaCl concentration was further examined to find the best condition. From this attempt with the fixed concentration of PEG 10,000 at 19% (w/v), larger protein crystals were obtained from the combination of 19% PEG 10,000, 20% (w/v) glycerol, 0.1 M Tris-HCl pH 8.5 and 0.1 M NaCl with 15 mg/ml protein concentration (Figure 19). Lower NaCl concentration leads the nucleation of many small protein crystals (Figure 20). The crystallization trial without NaCl in precipitant solution results in the cluster crystals (Figure 21).

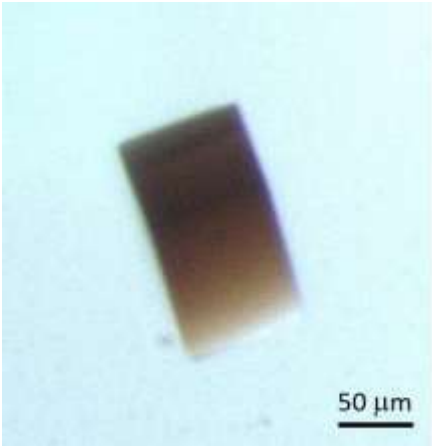

Figure 19. Crystals obtained by the optimization of the protein concentration. Initial screening conditions were further optimized. Larger and thicker protein crystals were obtained from the solution of 15 mg/ml protein and 19% (w/v) PEG10,000, 20% (w/v) glycerol, 0.1 M Tris-HCl pH 8.5 and 0.1 M NaCl.

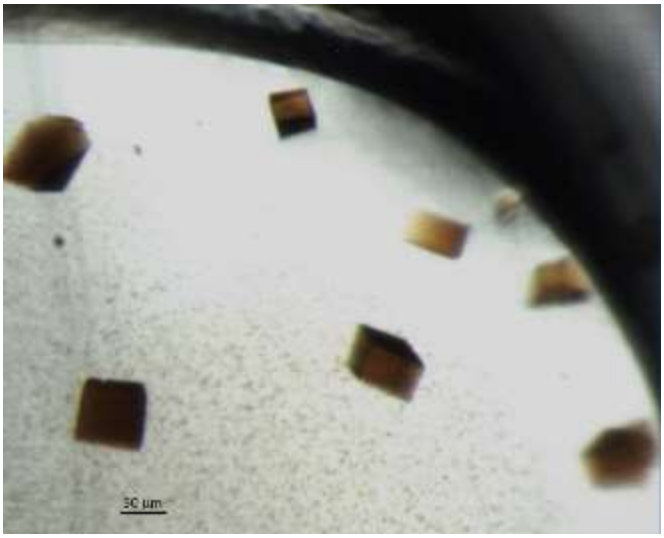

Figure 20. Crystals obtained at lower NaCl concentration.
Tiny crystals were obtained from the droplets consisting of 15 mg/ml of the protein and 19% (w/v) PEG10,000, 20% (w/v) glycerol, 0.1 M Tris-HCl pH 8.5 and 0.02 M NaCl.

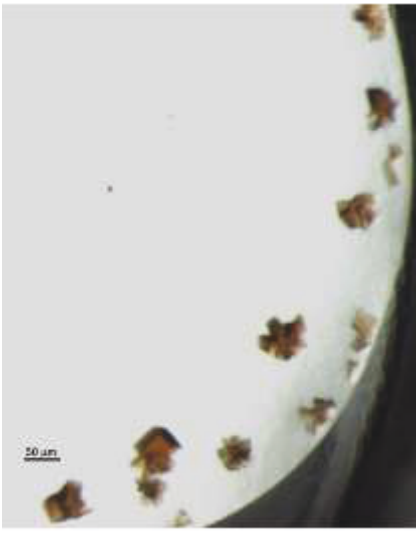

Figure 21. Crystals obtained from the solution without NaCl.
Clustered crystals were obtained from the droplets consisting of 15 mg/ml of the protein and 19% (w/v) PEG10,000, 20% (w/v) glycerol, 0.1 M Tris-HCl pH 8.5.

3.5 Data collection and processing

The X-ray diffraction data showed that the HYD2-s77 crystals belonged to the monoclinic space group $P2_1$ with unit cell parameters of a = 63.90, b = 118.89, c = 96.70 Å, β= 100.61 ° (with trypsin treatment), and a = 65.38, b = 121.45, c = 98.63 Å, β= 102.29 ° (without trypsin treatment). Data collection statistics are summarized in Table 8. The crystals from the samples with and without trypsin treatment diffracted to 1.60 and 2.00 Å (Figure 22), respectively, which indicates that the diffraction quality of the crystal was considerably improved by the trypsin treatment. Other statistic values, $R_{\text{r.i.m.}}$ and overall B factor, were also improved by the trypsin treatment. Based on the presence of two heterodimeric molecules in the asymmetric unit of the crystals from samples purified with and without trypsin treatment, the Matthews coefficients were calculated to be 2.01 and 2.13 $Å^3$ Da^{-1} with solvent contents of about 39% and 42%, respectively. Subsequently, the molecular replacement method was applied using the program Molrep from CCP4.

Table 8. Data collection and processing

Data set	HYD2-s77 with trypsin treatment	HYD2-s77 without trypsin treatment
Diffraction source (SPring-8)	BL44XU	BL44XU
Wavelength (Å)	0.9000	0.9000
Temperature (K)	100	100
Detector	MX300HE	MX300HE
Crystal-detector distance (mm)	160	190
Rotation range per image (°)	0.5	1.0
Total rotation range (°)	180	180
Exposure time per image (s)	0.5	1.0
Space group	$P2_1$	$P2_1$
a, b, c (Å)	63.90, 118.89, 96.70	65.38, 121.45, 98.63
α, β, γ (°)	90.00, 100.61, 90.00	90.00, 102.29, 90.00
Mosaicity (°)	0.59	0.53
Resolution range (Å)	28.75 - 1.60 (1.69 - 1.60)	33.68 - 2.00 (2.11 - 2.00)
Total No. of reflections	93446	51136
No. of unique reflections	26992	14294
Completeness (%)	99.9 (99.4)	98.7 (97.0)
Redundancy	3.7 (3.5)	3.7 (3.6)
$\langle I/\sigma(I) \rangle$	8.5 (3.3)	10.8 (3.0)
$R_{\mathrm{r.i.m.}}$	0.093 (0.478)	0.121 (0.414)
Overall B factor from Wilson plot (Å^2)	7.4	21.1

Values in parentheses are for the outer shell.

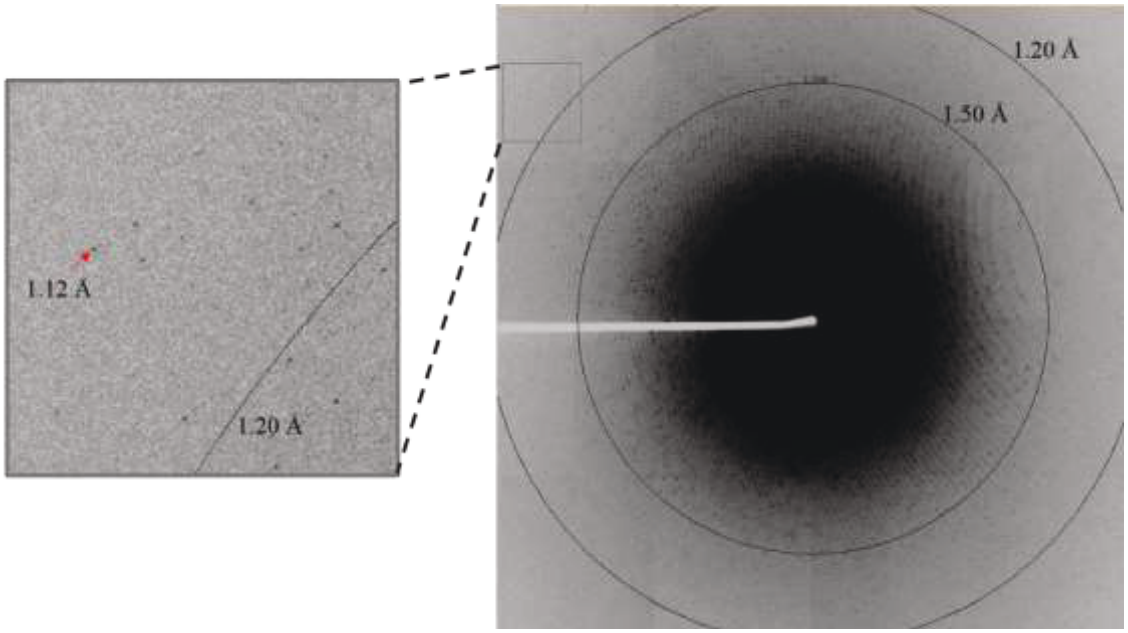

(*a*)

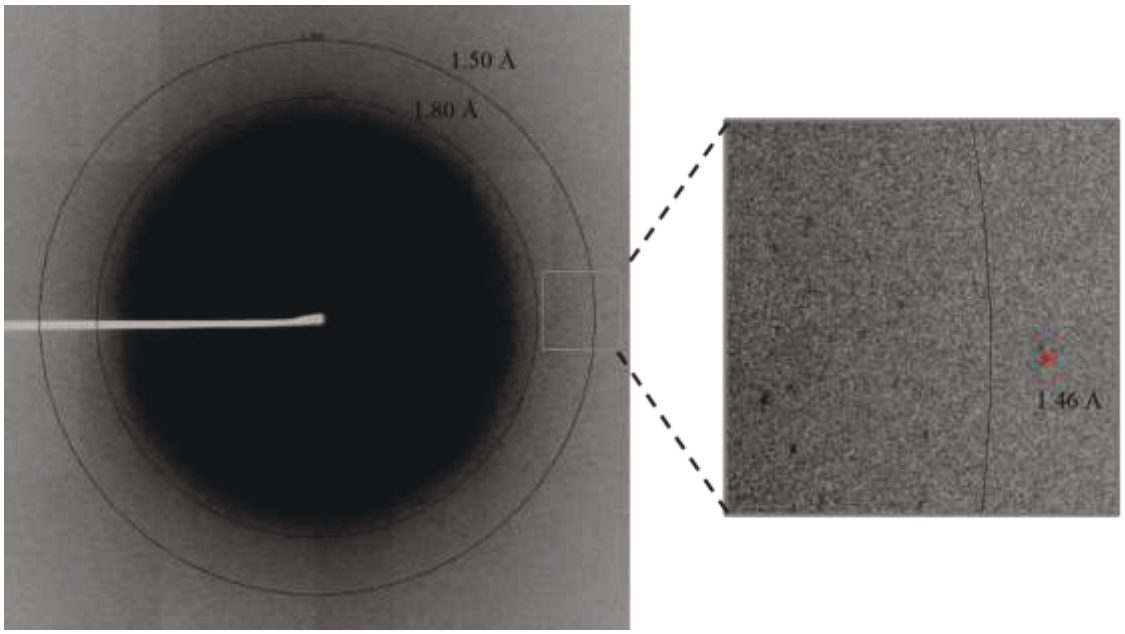

(*b*)

Figure 22. X-ray diffraction pattern from crystals of (*a*) HYD2-s77 with trypsin treatment, and (*b*) HYD2-s77 without trypsin treatment. The red arrow shows the highest resolution diffracted spot at 1.12 Å and 1.46 Å for (*a*) and (*b*), respectively.

4.0 Discussion

4.1 Purification of HYD2-s77

Overall purification results were summarized in Table 5. In both purification procedures with and without trypsin treatment after column chromatography, 5.37 mg and 3.92 mg of HYD2-s77 were obtained from 65.0 g of the bacterial cell pellets, respectively. The specific activity (580 U/mg) and recovery (49%) of the purified enzyme with trypsin treatment were better than those (233 U/mg and 13%) by only Triton X-100 treatment without trypsin, respectively (Table 5). The specific activity of the enzyme with trypsin treatment was 2.5 times higher than that without trypsin treatment, even though this was lower than the value (661 U/mg) reported in the original paper by Eguchi *et al*. (2012). The recovery, however, was considerably improved from 16.3 to 48.5% with trypsin treatment. Protein impurities were reduced in purification treated with trypsin as shown by SDS-PAGE (Figure 14(*d*)). An extra band around 70 kDa was successfully removed in the final step of the hydrophobic chromatography. However, the molecular mass difference caused by the elimination of the N- and/or C-terminus of HYD2-s77 with trypsin treatment was hardly recognized from SDS-PAGE analysis.

These results clearly showed that the trypsin treatment was effective for getting a sufficient amount of the protein sample in high purity for further crystallization screenings.

4.2 Oxygen tolerant property

Oxygen tolerant property of HYD2-s77 was investigated by using TTC as an artificial electron acceptor from the enzyme. TTC salts are colourless compounds which become coloured when reduced to TPF (Butcher & Altman, 1973). Reduction of TPF is irreversible and the intensity of the coloured TPF is proportional to the enzyme activity which can be quantified using spectrophotometry.

Oxygen tolerant property of HYD2-s77 was compared with three [NiFe]-hydrogenases, STD-dvm and MBH-mar, as a benchmark for O_2- sensitive and O_2-tolerant hydrogenases, respectively. In this experiment, STD-dvm, the typical standard [NiFe]-hydrogenase,

showed a strong H_2-consumption activity without O_2, but the activity could not be recovered in the presence of a small amount (4.2 nmol) of O_2 (Figure 15(*b*)). HYD2-s77 showed a relatively prolonged lag time for the various O_2 concentrations compared with MBH-mar, but the activity was recovered in the presence of 63.0 nmol of O_2 (Figure 15(*c*)). Upon exposure to O_2, the Ni-Fe active site of the standard [NiFe]-hydrogenases is converted into two inactive forms, Ni-A and Ni-B, where an oxygenated ligand bridges Ni and Fe (Hamdan *et al*., 2012). The oxygen tolerant hydrogenase is privileged by their ability to form only Ni-B which is reactivated much quickly than Ni-A in the standard hydrogenases. The results presented In Figure 15 demonstrate that HYD2-s77 also retained catalytic activity toward H_2 consumption in the presence of some amount of O_2 suggesting that HYD2-s77 forms Ni-B state upon O_2 exposure. It also demonstrates that HYD2-s77, one of the Hyd2-type enzymes, has an obvious O_2 tolerance.

4.3 Crystallization

Highly purified fractions from final step chromatography were further dialyzed to remove trace of the residual ammonium sulfate in the protein sample. Optimization was performed by varying the protein and PEG10,000 concentrations by using the grid screens method (Figure 5 and 6).

Best crystals for protein with and without trypsin treatment were obtained from the condition containing 18% (w/v) and 19 % (w/v) of PEG10,000 with 11 mg/ml and 15 mg/ml of the protein, respectively. (Figures 17 and 19). These two conditions showed good reproducibility to get larger crystals in better quality than the other conditions.

Function of precipitants in the crystallization drop is to alter the protein-solvent or protein-protein contacts so that protein molecules precipitates out of solution, preferably in a way of ordered crystals (Bergfors, 1999). Polyethylene glycol 3,350 (PEG 3,350), PEG 4000 and PEG 8000 are the most widely used chemicals in protein crystallization recorded in PDB (Kirkwood *et al*., 2015). In case of HYD2-s77, PEG 10,000 works best as the precipitant.

Differential scanning fluorimetry has shown that proteins are stabilized by moderate concentrations of salt in their buffer formulations (Ristic *et al*, 2015). At lower NaCl concentration with combination of 19% (w/v) PEG 10,000 results in smaller size and clustered protein crystals (Figure 20 and 21). Increased salt concentration may stabilize the protein solution (potentially allowing the protein concentration to be increased) or decrease the protein solubility which affects the precipitation. Concentration of salt also is assumed to affect the hydration shell around the protein, which may facilitates the protein-protein interactions that necessary to drive nucleation and crystallization (Zhang and Cremer, 2006).

For both crystallization attempts, besides the precipitant concentration, the protein concentration is also important parameter that affects the crystal growth. Higher protein concentration in the drop may trigger extra nucleation or even precipitation which should be avoided. In addition, crystallization temperature was also important parameter. The best crystals were consistently obtained at 10°C, whereas crystallization at 4°C always results in precipitation and/or microcrystals.

4.4 Data collection and processing

As shown in Table 8, diffraction quality of the crystal was considerably improved by the trypsin treatment. Other statistic values, $R_{\text{r.i.m.}}$ and overall B factor, were also improved. These values are directly related to the high homogeneity of the purified sample with trypsin treatment. This may cause by the evenly trimmed structure of the long C-terminal loop of the small subunit of HYD2-s77. The cleaved protein part may be usually eliminated during purification. Therefore, it is suggested that high homogeneity of the target protein sample significantly improved the crystal packing.

5.0 Conclusions

The purification procedure of HYD2-s77 was improved by applying a treatment of trypsin before chromatography. Both the purified protein samples with and without trypsin treatment were successfully crystallized by using the sitting drop vapor diffusion method and polyethylene glycol as a precipitant at 10° C. Both crystals belonged to the space group $P2_1$. The crystals obtained from trypsin treatment diffracted to 1.60 Å, which is considerably improved than the 2.00 Å resolution obtained without trypsin treatment. This work also showed that [NiFe]-hydrogenase from *Citrobacter* sp. S-77 still retained its catalytic activity with some amount of O_2 even though it is from Hyd-2 type [NiFe]-hydrogenase. This indicates that HYD2-s77 has a clear O_2 tolerance.

6.0 Future plans

Structure elucidation for HYD2-s77 in reduced, air-oxidized and superoxidized form need to be carefully elucidated in order to establish a unique structure-function of this enzyme. In addition, higher resolution of X-ray diffraction results will be very informative to solve the proton transfer pathway between catalytic center to the surface of the protein enzyme. Although [NiFe]-hydrogense have been extensively characterized by X-ray crystallography, and many different chemical states have been recognized by infrared spectroscopy, many questions still remain about the identity and structure of the ligand species involve in [NiFe]-hydrogenase. Spectroscopic studies are very helpful to determine the different redox states of the active site in the catalytic, activation/deactivation and light-induced processes of HYD2-s77 for these information can provide the difference of electronic structure between O_2-tolerant Hyd-1-type, O_2-tolerant Hyd-2-type and standard [NiFe]-hydrogenase. Furthermore, identity of any ligand species involves in the catalytic center and redox chain in HYD2-s77 should be addressed in order to find out why HYD2-s77 is oxygen tolerant even though it is Hyd-2-type hydrogenase. Besides, spectroscopic method and electrochemical studies on HYD2-s77 are good combination to characterize the structure, electronic and coordination changes in the protein molecules.

7.0 References

Bergfors, T.M. (1999). "Protein crystallization techniques, strategies, and tips: A laboratory manual", published by International University Line, La Jolla, CA, USA, pp. 41-50.

Butcher, R.G. & Altman, F.P. (1973). Studies on the Reduction of Tetrazolium Salts. *Histochemie*. **37**, 351-363.

Chenevier, P, Mugherli, L., Darbe, S., Darchy, L., DiManno, S., Tran, P.D., Valentino, F., Iannello, M., Volbeda, A., Cavazza, C., Artero, V. (2013). Hydrogenase enzymes: Application in biofuel cells and inspiration for the design of noble-metal free catalyst for H_2-oxidation. *C.R. Chimie*. **16**, 491-505.

Collaborative Computational Project, Number 4, (1994). The CCP4 suite: programs for protein crystallography. *Acta Cryst. D*. **50**, 760-763.

Cracknell, J. A., Wait, A.F., Lenz, O., Friedrich, B. & Armstrong, F.A. (2009). A kinetic and thermodynamic understanding of O_2 tolerance in [NiFe]-hydrogenases. *Proc. Natl. Acad. Sci.* **106**, 20681-20686.

Eguchi, S., Yoon, K.-S. & Ogo, S. (2012). O_2-stable membrane-bound [NiFe] hydrogenase from a newly isolated *Citrobacter* sp. S-77. *J. Biosci. Bioeng*. **114**, 479-484.

Evans, P. (2006). Scaling and assessment of data quality *Acta Cryst. D.* **62**, 72-82.

Fritsch, J., Scheerer, P., Frielingsdorf, S., Kroschinsky, S., Friedrich, B., Lenz, O. & Spahn, C.M.T. (2011). The crystal structure of an oxygen-tolerant hydrogenase uncovers a novel iron-sulphur centre. *Nature (London)*. **479**, 249-252.

Goris, T., Wait, A. F., Saggu, M., Fritsch, J., Heidary, N., Stein, M., Zebger, I., Lendzian, F., Armstrong, F. A., Friedrich, B. & Lenz, O. (2011). A unique iron-sulfur cluster is crucial for oxygen tolerance of a [NiFe]-hydrogenase. *Nat. Chem. Biol.* **7**, 310–318.

Hamdan, A.A., Liebgott, P.-P., Fourmond, V., Gutierrez-Sanz, O., De Lacey, A.L., Infossi, P., Rousset, M., Dementin, S., Leger, C. (2012). Relation between anaerobic inactivation and oxygen tolerance in a large series of NiFe hydrogenase mutants. *Proc. Natl Acad. Sci. USA.* **109**, 19916-19921.

Higuchi, Y., Yasuoka, N., Kakudo, M., Katsube, Y., Yagi, T. & Inokuchi, H. (1987). Single crystals of hydrogenase from *Desulfovibrio vulgaris* Miyzaki F. *J. Biol. Chem.* **262**,

2823-2825.

Hocking, M.B. (1998) “Handbook of Chemical Technology and Pollution Control” published by Academic Press, California, USA, pp.109-113.

Kirkwood, J., Hargreaves, D., O’Keefe, S. & Wilson, J. (2015). Analysis of crystallization data in the Protein Data Bank. *Acta Cryst. F.* **71**, 1228-1234.

Lubitz, W., Ogata, H., Rüdiger, O. & Reijerse, E. (2014). Hydrogenases. *Chem. Rev*. **114**, 4081-4148.

Lukey, M.J., Parkin, A., Roessler, M.M, Murphy, B.J., Harmer, J., Palmer, T., Sargent, F. & Armstrong, F.A. (2010). How *Escherichia coli* is equipped to oxidized hydrogen under different redox conditions. *J. Biol. Chem.* **285**, 3928-3938.

Matsumoto, T., Eguchi, S., Nakai, H., Hibino, T., Yoon, K.-S. & Ogo, S. (2014). [NiFe] hydrogenase from *Citrobacter* sp. S-77 surpasses platinum as an electrode for H_2 oxidation reaction. *Angew. Chem. Int. Ed*. **53**, 8895-8898.

Mertens, R. & Liese, A. (2004). Biotechnological applications of hydrogenases. *Curr. Opin. Biotechnol*. **15**, 343-348.

Ogata, H., Lubitz, W. & Higuchi, Y. (2009). [NiFe] hydrogenases: structural and spectroscopic studies of the reaction mechanism. *Dalton Trans*. **37**, 7577-7587.

Pandelia, M.-E., Nitschke, W., Infossi, P., Giudici-Orticoni, M., Bill, E. & Lubitz, W. (2011). Characterization of a unique [FeS] cluster in the electron transfer chain of the oxygen tolerant [NiFe] hydrogenase from *Aquifex aeolicus*. *Proc. Natl Acad. Sci. USA* **108**, 6097–6102.

Ristic, M., Rosa, N. Seabrook, S.A. & Newman, J. (2015). Formulation screening by differential scanning fluorimetry: how often does it work?. *Acta Cryst. F***. 71**, 1359-1364.

Shomura, Y., Yoon, K.-S., Nishihara, H. & Higuchi, Y. (2011). Structural basis for a [4Fe-3S] cluster in the oxygen tolerant membrane-bound [NiFe]-hydrogenase. *Nature (London)*. **479**, 253-256.

Vignais, P.M., Billoud, B., Meyer, J., (2001). Classification and phylogeny of hydrogenases. *FEMS Microbiol. Rev*. **25**, 455-501.

Vignais, P.M. & Billoud, B. (2007). Occurrence, classification, and biological function of hydrogenases: An Overview. *Chem. Rev.* **107**, 4206-4272.

Volbeda, A., Charon, M.-H., Piras, C., Hatchikian, E.C., Frey, M. & Fontecilla-Camps, J.C. (1995). Crystal structure of the nickel-iron hydrogenase from *Desulfovibrio gigas*. *Nature*. **373**, 580-587.

Yagi, T., Endo, A. & Tsuji, K. (1978). "Hydrogenases: Their Catalytic Activity, Structure and Function" ed. by Schlegel, H.G. and Schneider, K., published by Erich Goltze, Göttingen, pp. 107-124

Yoon, K-S., Fukuda, K., Fujisawa, K. & Nishihara, H. (2011). Purification and characterization of a highly thermostable, oxygen-resistant, respiratory [NiFe]-hydrogenase from a marine, aerobic hydrogen-oxidizing bacterium. *Int. J. Hydrogen Energ*. **36**, 7081-7088.

Zhang, Y. & Cremer, P.S.(2006). Interactions between macromolecules and ions: The Hofmeister series. Curr. Opin Chem Biol. **10**, 658-63.

Acknowledgement

I am deeply grateful to Professor Yoshiki Higuchi for his constant supervision of the project, fundraising and also for his constructive criticisms on my work which have always been both motivating and inspiring.

I also would like to thank Assistant Professor Koji Nishikawa of Higuchi Laboratory for his kind advice and valuable suggestions. I would like to extend my heartfelt gratitude to Associate Professor Naoki Shibata of Higuchi Laboratory and Associate Professor Yasuhito Shomura in Ibaraki University for their valuable suggestions, helpful discussions and support of X-ray data collection.

I am most grateful for having worked with an outstanding staff of Higuchi Laboratory who helped me in various occasions to get a better understanding of many questions which have arisen during the project. I also want to thank all laboratory member for their support on technical part.

I am also thankful to Leading Program in Doctoral Education of Graduate School of Life Science, University of Hyogo (Next-Generation Picobiology Pioneered by Photon Sciences) for its outstanding educational curriculum and funding my PhD research in part.

Finally, my biggest gratitude and appreciation to my beloved family, especially my dear parents who never stopped supporting and encouraging me over the years. Thanks too, to all my friends for the support for all these years. Thank you, all.